

Pre-Lab

All diagrams were created using Miro

- 1.) Quadrature Amplitude Modulation benefits from its high spectral efficiency. QAM can transmit significantly more data within a given frequency bandwidth by carrying bits in both amplitude and phase. Using two carrier waves (same frequency), but 90 degrees out of phase with each other (In-Phase 'I' or Quadrature 'Q' signals). By changing the amplitude of the I and Q signals, QAM creates a set of states – either 16, 64, or 256-QAM. It is able to switch between these states in order balance data transfer and reliability.
QAM is primarily used for digital data and is used to maximize data rate whereas Single-Sideband transmission is used primarily for analog signals where maximizing bandwidth and power efficiency is the goal.
- 2.) The drawback of using QAM is its susceptibility to noise and interference. This is even more prevalent with higher order signals like 256-QAM which require clean signals with high signal to noise ratios. It could also be seen as a downside that QAM requires a linear power amplifier since it stores information in the signals amplitude as well – resulting in the signals power level constantly changing. Additionally, QAM requires a receiver that can handle detecting small changes in amplitude and phase (simultaneously). The receiver needs to be synchronized with the transmitter's carrier frequency and phase, where any drift may corrupt the signal. In short, QAM requires more complexity and higher cost.

3.)

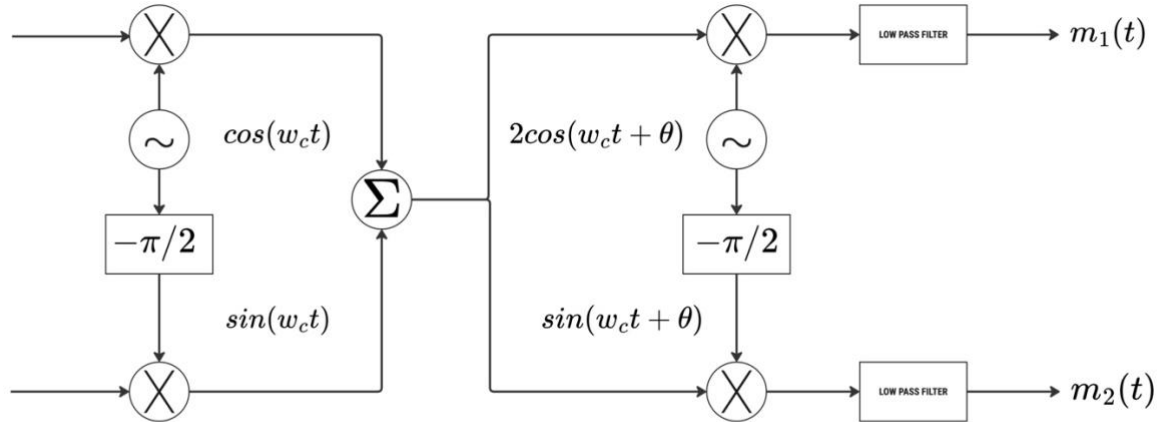


Figure 1: Demodulator with phase shift of theta

4.)

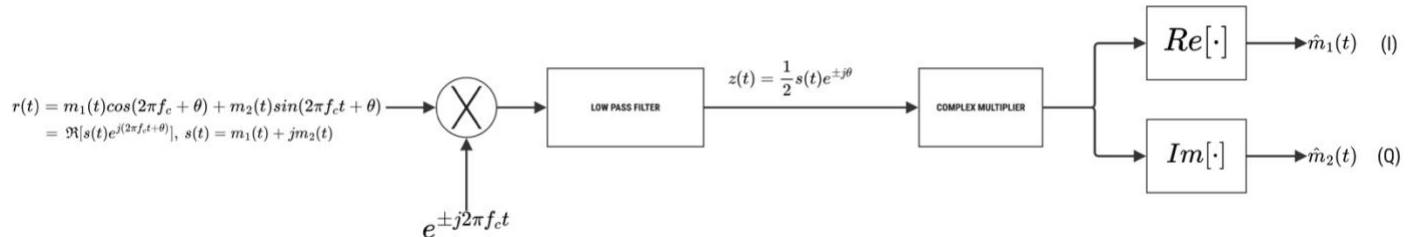


Figure 2:Coherent demodulator receiving a QAM signal

For part 6 we have the block diagram (Fig.3) where the transmitter side generates two baseband tones (200 Hz and 300 Hz) and upconverts them to a 15 kHz passband using orthogonal carriers with a common initial phase of $\pi/4$. The DSB-SC branches are summed together along with a noise block. On the receiver side, the real passband signal is converted to complex with Float-to-Complex. The frequency sink is connected at the float-to-complex output, to show the spectrum of the received QAM signal as it arrives at the RX. The spectrum in Fig. 4 shows a noisy passband centered at ± 15 kHz with two narrow sidebands around each carrier corresponding to the 200 Hz and 300 Hz messages. Because the RX signal is still passband and real the spectrum is evenly mirrored about 0 Hz. As expected, the carrier placement is at 15 kHz with the correct modulation (two symmetric sidebands), and the expected impact of channel noise prior to any coherent demodulation.

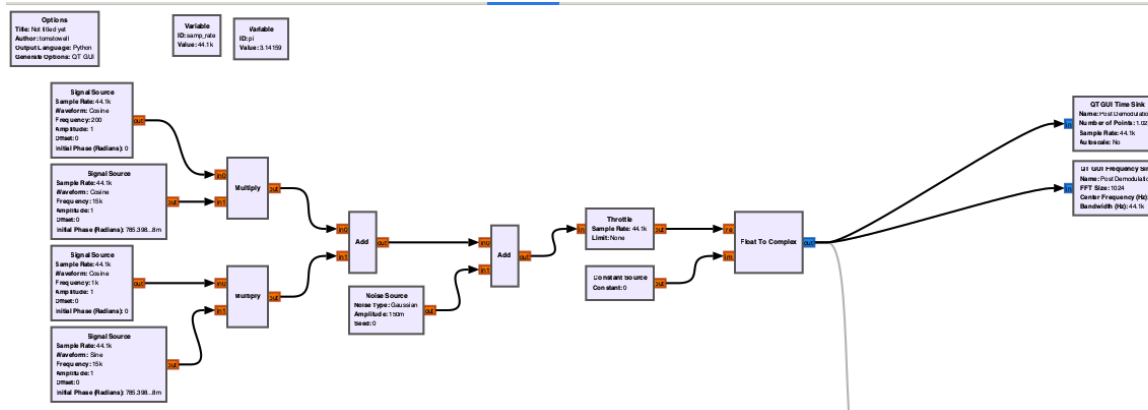


Figure 3: Block Diagram for problem 6

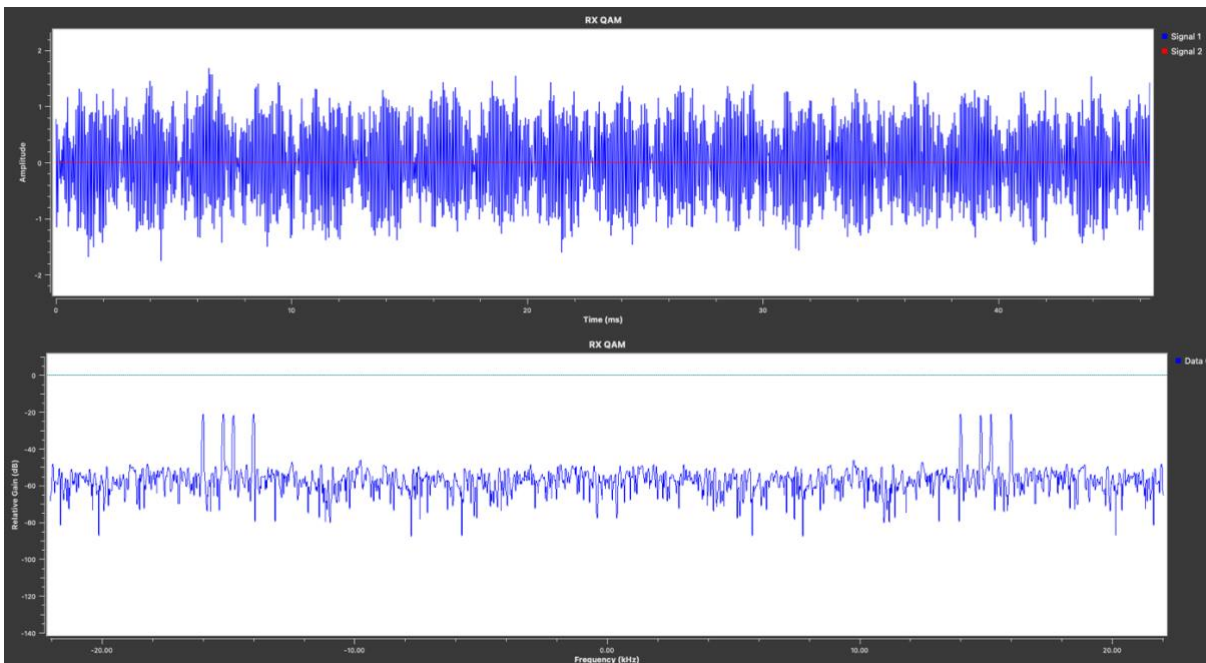


Figure 4: Time and spectral output from block diagram in figure 3

The complex coherent RX for QAM demod block diagram is shown in Fig. 5. After the real, noisy passband at the RX we added in a complex LO (reference carrier) and a multiplier to output the baseband I+jQ along with a low pass filter to remove high frequency images from the input. Fig. 6 shows the time and spectral output at the output of the low pass filter. In the time domain we have the real and imaginary channels showing low frequency sinusoids, which are the demodulated messages (200 Hz and 300 Hz) with noise. In the frequency domain, the spectrum is now centered at 0Hz with some spikes around ± 200 Hz and ± 300 Hz.

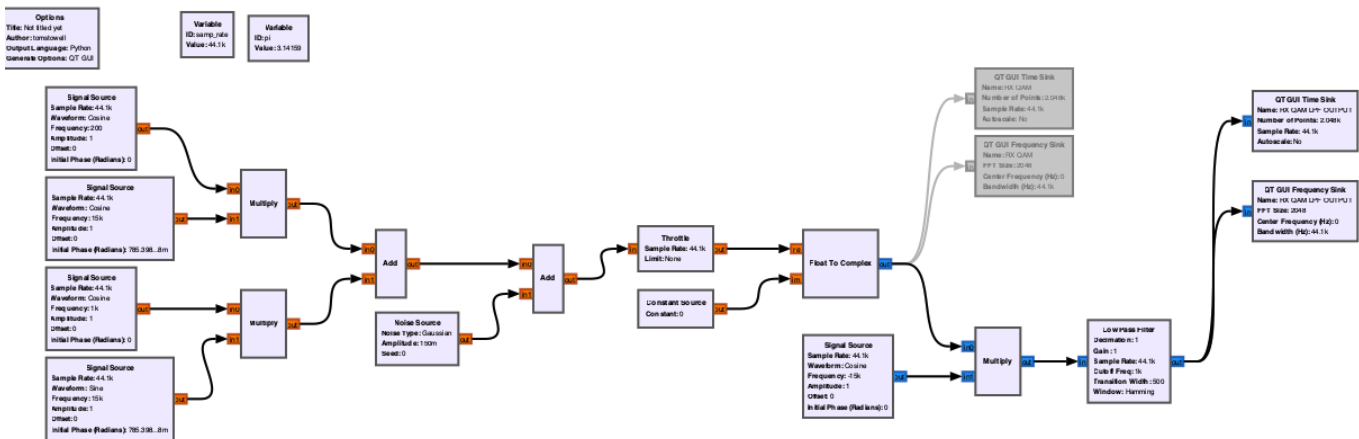


Figure 5: Block diagram for problem 7

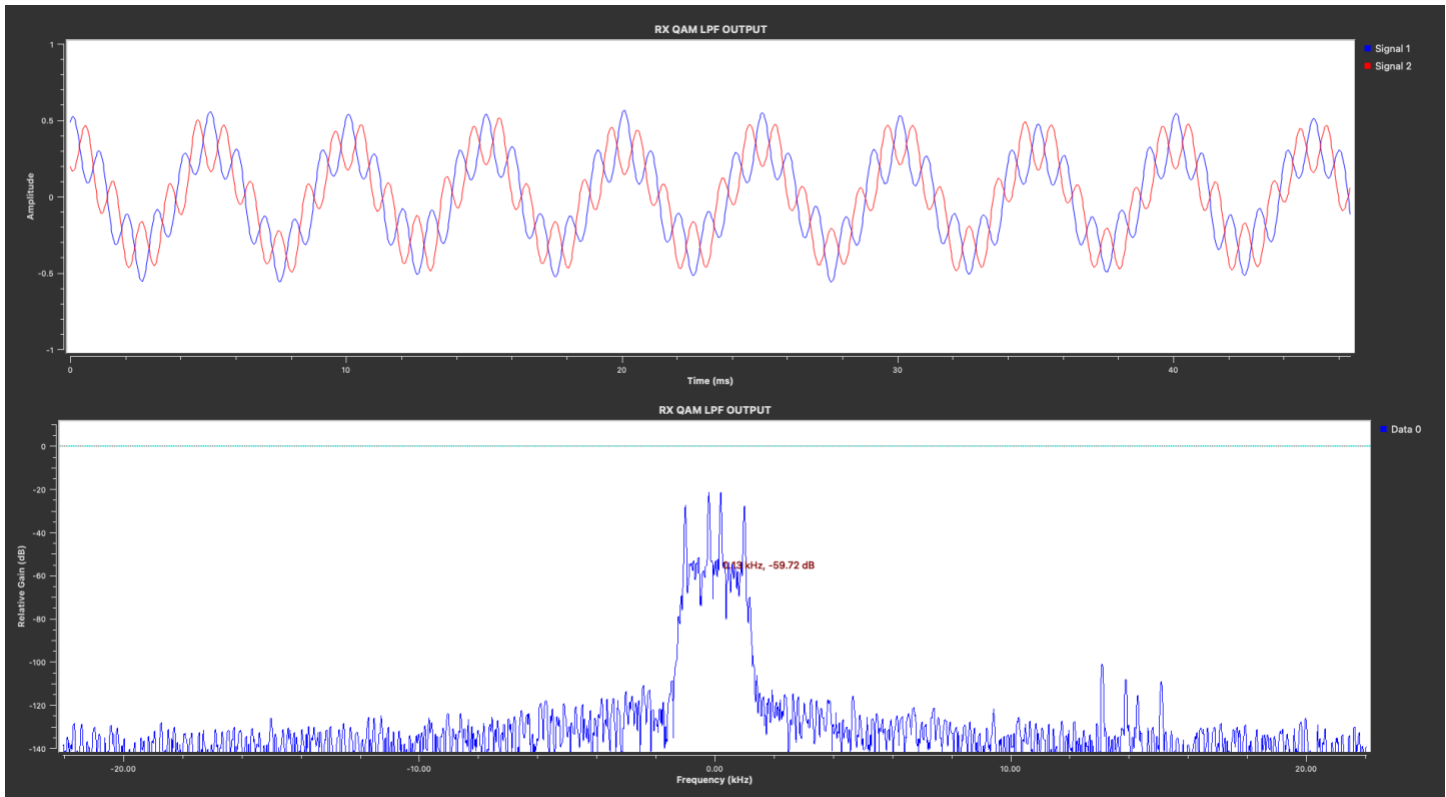


Figure 6: Time and spectral plots from block diagram in figure 5

The graph in Fig. 7 adds coherent demodulation and a tunable phase correction by adding a signal source that acts as a phase rotator. All the plots (Figs. 8-11) are share a centered 0 Hz with lines at ± 200 Hz and ± 300 Hz in the frequency sink, two signals in the time sink (Signal 1 = Real (I), Signal 2 = Imag(Q)) and constellation sink where its orientation depends on φ . Fig. 8 shows no phase correction ($\varphi = 0$), where I and Q each show a mixture of 200 Hz and 300 Hz. The RX LO has phase 0 while TX carriers had $+\pi/4$, so the I/Q basis is rotated. So, without phase correction the I/Q axes are rotated. Fig. 9 shows TX phase correction by setting $\varphi = -\pi/4$. The channels separate in the time plot where $I \approx 200$ Hz and $Q \approx 300$ Hz, so each channel looks like a clean sinusoid. In the frequency domain we have the same $\pm 200/\pm 300$ Hz lines, but now each line predominantly appears in one channel. And the ellipse aligns with axes in the constellation plot. This is the correct coherent demod setting for the link. Fig.10 shows a 90° phase shift (φ correct + 90°) where I/Q swap in the time domain (I now looks like 300 Hz, Q like 200 Hz). We can see the ellipse rotate by 90 degrees in the constellation plot. And finally in Fig. 11, we have a 180° phase shift (φ correct + 180°). In the time domain both channels look like the correct case but phase reversed and the ellipse is rotated by 180° in the constellation plot.

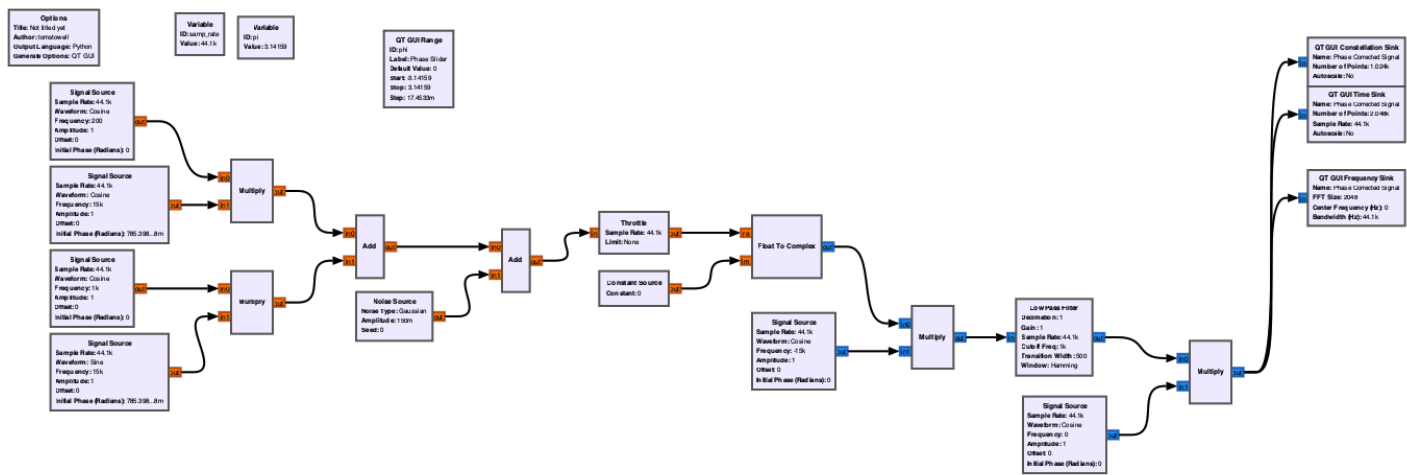


Figure 7: Block diagram with coherent demodulation and a tunable phase correction

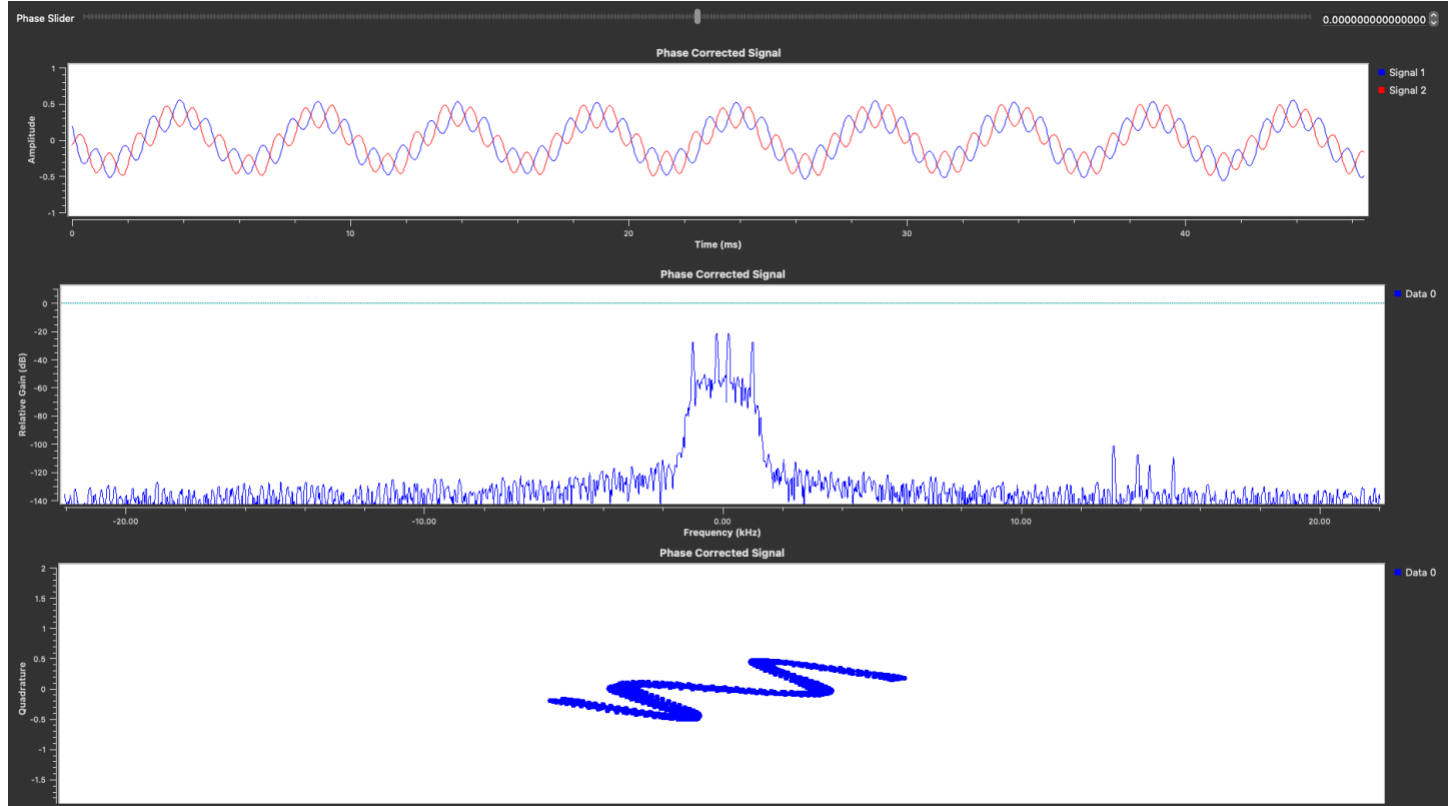
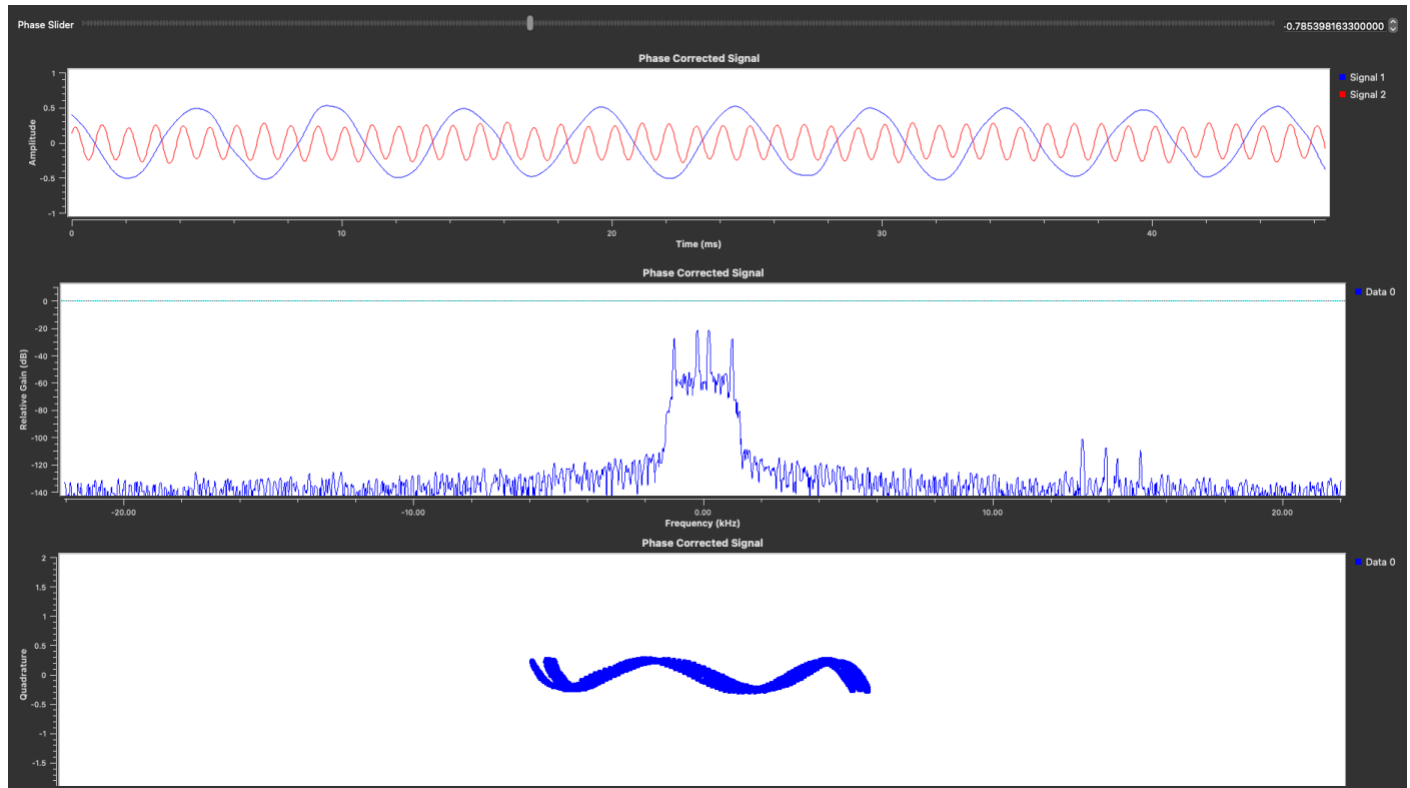
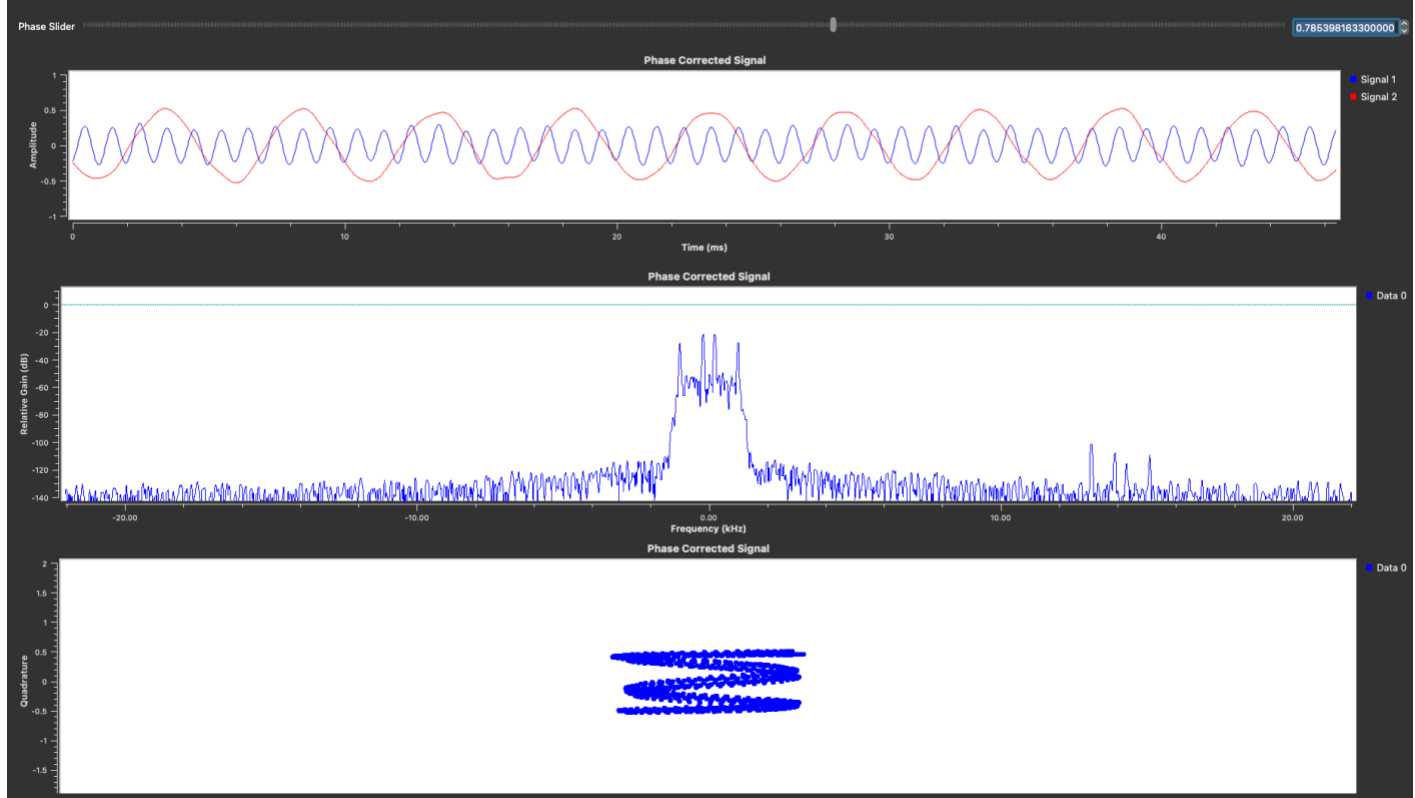
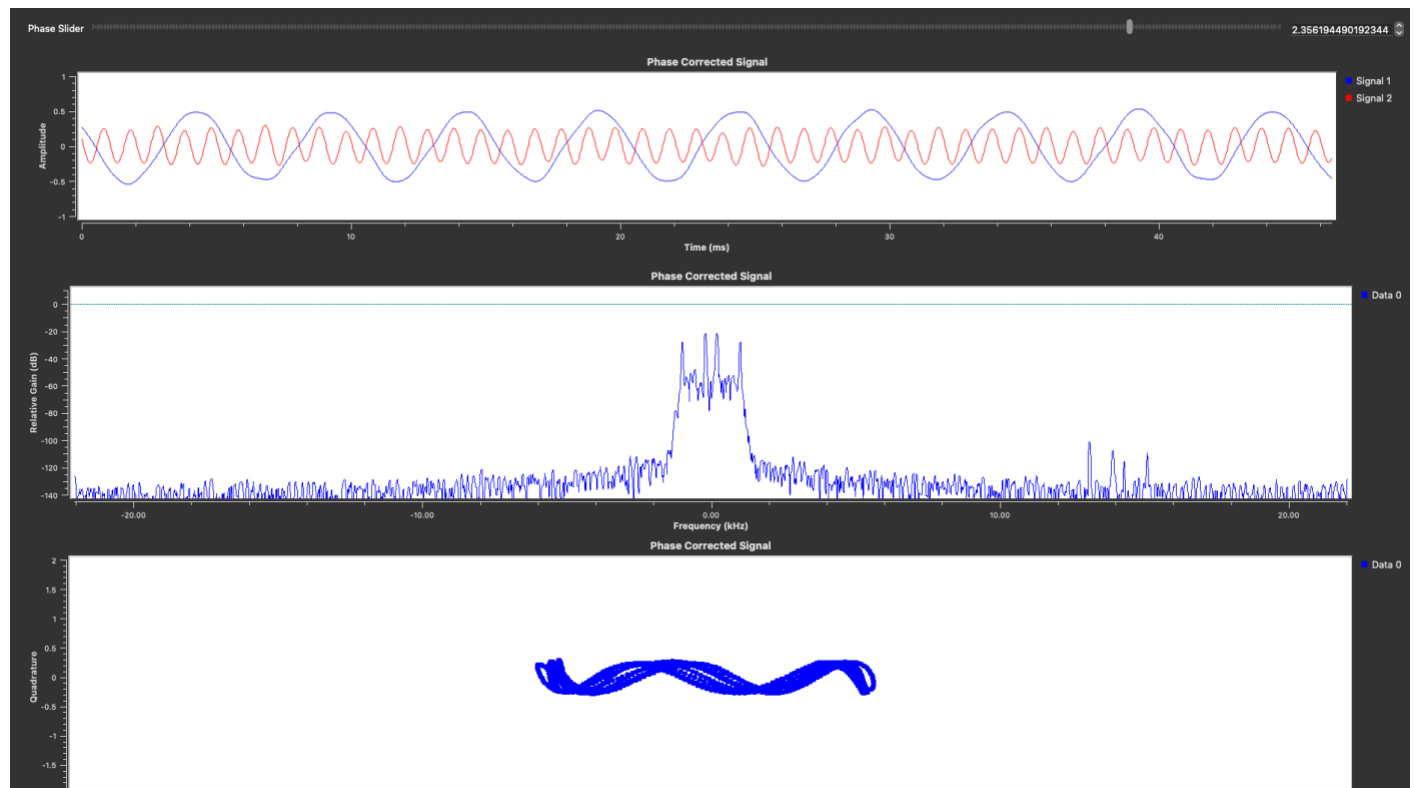


Figure 8: No phase correction

Figure 9: Phase correction $\phi = -\pi/4$

Figure 10: Phase shift $\phi = \pi/4$ Figure 11: Phase shift $\phi = 3\pi/4$